Applied Physics A (2019) 125:482
https://doi.org/10.1007/s00339-019-2777-4

Applied Physics A
Materials Science & Processing

Study on gamma-ray buildup factors of bismuth borate glasses

Mohammed Sultan Al-Buriahi[1] · **Baris T. Tonguc**[1]

Received: 5 May 2019 / Accepted: 27 June 2019 / Published online: 29 June 2019

Abstract

Energy absorption buildup factor (EABF) and exposure buildup factor (EBF) of bismuth borate glass systems in structure (75–x)B_2O_3–xBi_2O_3–10Na_2O–10CaO–5Al_2O_3 ($0 \leq x \leq 25$ mol%) have been investigated for photon energy region between 0.015 and 15 MeV and for penetration depths of 1–40 mfp. Five parameters (G–P) fitting method has been carried out for computations procedure. The calculated values of EABF and EBF have been observed to be dependent on photon energy, penetration depths and on the concentration of Bi_2O_3 mol% in the glass sample. It has been found that BOB25 glass offers better gamma-ray shielding than other samples. In addition, the values of EABF and EBF have been compared and significant differences up to 8% have been noted in intermediate energy region.

1 Introduction

Radiation shielding guarantees that people can work safely in an environment, where ionizing radiation occurs whether this is in a hospital, laboratory, nuclear power plants, or nuclear waste treatment location. Concrete protects the environment properly against gamma ray. However, there are still limitations associated with their use [1, 2]. Glasses, especially those doped with heavy metal oxide, offer an excellent alternative shielding material against gamma ray [3–5]. This triggered much interest for investigation of gamma-ray shielding features for different types of glasses [6–10].

In the literature, many studies focused on manufacturing novel developed glasses or new glass systems [11–13]. Other studies devoted their efforts to study the gamma interaction properties of those glasses [14, 15]. Gamma–glass interaction can be investigated by Lambert's Beer law. According to this law, the gamma source should be monoenergetic beam associated with narrow beam setup and thin slab of the studied sample [16, 17]. If any one of mentioned conditions is not met, then a correction term called "buildup factor (BUF)" has to add to Lambert's Beer law. The BUF is related to the absorbed energy in medium or in the air. In the first case, the BUF is called energy-absorption buildup factor (EABF), and in the other case, the BUF is called exposure buildup factor (EBF) [18, 19]. More knowledge about EABF and EBF was reported in detail by American Nuclear Society (ANSI/ANS) [20].

The BUF can be obtained using (G–P) fitting method. The accuracy of this method was tested by several authors. Singh et al. evaluated the exposure buildup factors for bismuth borosilicate glasses and he found that these glasses have superior gamma-ray shielding properties comparing with steel–magnetite concrete and lead [17]. Esra et al. calculated EABF and EBF of lithium borate glasses doped with minerals and the results revealed that the addition of minerals in glasses improves the gamma-ray shielding features [21]. Moreover, EABF and EBF have been investigated using the method of invariant embedding for 26 materials up to depths of 100 mfp [22]. Finally, Monte Carlo simulation method is also utilized to estimate gamma-ray buildup factors for different materials [23, 24].

Very recently, bismuth borate glasses in composition (75-x)B_2O_3–xBi_2O_3–10Na_2O–10CaO–5Al_2O_3 ($0 \leq x \leq 25$ mol%) were prepared using the melt-quenching method [12]. Gamma-shielding properties of this glass systems were investigated in terms of mass attenuation coefficient, effective atomic number, and HVL [25]. A full understanding of these glasses is has to be achieved by determination gamma-ray buildup factors and this has prompted us to carry out the present study. In this study, the buildup factors (EABF and EBF) of the bismuth borate glasses have been evaluated using (G–P) fitting meothd over a wide range of energy (0.015–15 MeV) and up to 40 mfp. A comparison between EABF and EBF has also been reported in the present work.

✉ Mohammed Sultan Al-Buriahi
mburiahi@gstd.sci.cu.edu.eg;
mohammed.al-buriahi@ogr.sakarya.edu.tr

[1] Department of Physics, Sakarya University, Sakarya, Turkey

The study provides helpful results to design bismuth borate glasses for many protection applications against gamma ray.

2 Materials and methods

Bismuth borate glasses in the aforementioned chemical composition (Table 1) have been prepared using the melt-quenching technique [12]. High-purity oxides such as H_3BO_3, Na_2CO_3, $CaCO_3$, Al_2O_3, and Bi_2O_3 have been utilized. These oxides have been melted, stirred in alumina crucibles at about 900–1000 °C (30–40), and poured. This glass has been then annealed at 400 °C in another oven for 1 hour, and after that, it was cooled for 24 h. Table 1 shows the elemental weight fraction, density, and the sample code of the chosen glass systems.

The BUFs have been calculated from the G–P-fitting parameters that have been generated using the interpolation method for the equivalent atomic number (Z_{eq}). The calculation proceedings of gamma-ray buildup factors (EABF and EBF) can be divided into three steps [26, 27]:

2.1 Calculation of Z_{eq}

Z_{eq} is a parameter that has a similar meaning of the atomic number of a single element. However, the equivalent atomic number unlike the atomic number depends on the photon energy. To find Z_{eq}, we have calculated the ratio of Compton mass attenuation coefficient $(\mu_m)_{Comp}$ and the total mass attenuation number $(\mu_m)_{total}$ for the given glass in the energy range 0.015–15 MeV using WinXCom program [28]. Then, the Z_{eq} values have been obtained by interpolation method by matching the previous ratio of the selected glasses with the identical ratio of a pure element at the same energy. The following equation has been used to interpolate Z_{eq}:

$$Z_{eq} = \frac{Z_1(\log R_2 - \log R) + Z_2(\log R - \log R_1)}{\log R_2 - \log R_1}, \quad (1)$$

where Z_1 and Z_2 are the atomic numbers corresponding to the ratio R_1 and R_2, respectively. R is the ratio of the given glasses at specific energy.

2.2 Evaluation of the G–P-fitting parameters

The calculated Z_{eq} values for the glasses have been used to obtain the G–P-fitting parameters (b, c, a, X_K and d) using the formula [29, 30]:

$$P = \frac{P_1(\log Z_2 - \log Z_{eq}) + P_2(\log Z_{eq} - \log Z_1)}{\log Z_2 - \log Z_1}, \quad (2)$$

where P_1 and P_2 are the G–P-fitting parameters corresponding to the atomic numbers Z_1 and Z_2, respectively. Such those parameters were reported for 26 elements, water, and air by American Nuclear Society [20].

2.3 Calculation of gamma-ray buildup factors

The calculation of EABF and EBF for the present glasses has been done using the G–P-fitting parameters as follows [31, 32]:

$$B(E,X) = 1 + \frac{b-1}{K-1}(K^x - 1) \quad \text{for} \quad K \neq 1, \quad (3)$$

$$B(E,X) = 1 + (b-1)x \quad \text{for} \quad K = 1, \quad (4)$$

where

$$K(E,X) = cx^a + d\frac{\tanh\left(\frac{x}{X_k} - 2\right) - \tanh(-2)}{1 - \tanh(-2)} \quad \text{for} \quad x \leq 40, \quad (5)$$

where E is the photon energy, x is the penetration depth in mfp, and $K(E, X)$ is the dose-multiplicative factor.

3 Standardization of computational method

The method described in Sect. 2 has been standardized by calculating the EABF for water and comparing the obtained results with those of American National Standards [20]. The comparison has been done over a wide range of photon energies (0.015–15 MeV) and at different penetration depths 1, 5, 10, 20, and 40 mfp. We have provided the compared values of EABF in Fig. 1 and good agreement has been

Table 1 Elemental weight fraction, density, and the glass code of the chosen glass systems

Glass code	B	O	Na	Al	Ca	Bi	Density (g/cm^3)
BOB00	0.234618	0.601839	0.066522	0.039036	0.057984	0	2.25
BOB05	0.170183	0.467736	0.051700	0.030338	0.045064	0.234979	2.938
BOB10	0.129232	0.382505	0.042279	0.024810	0.036852	0.384322	3.572
BOB15	0.100904	0.323548	0.035762	0.020986	0.031172	0.487628	4.269
BOB20	0.080143	0.280338	0.030986	0.018183	0.027009	0.563340	4.509
BOB25	0.064273	0.247310	0.027336	0.016041	0.023827	0.621213	5.035

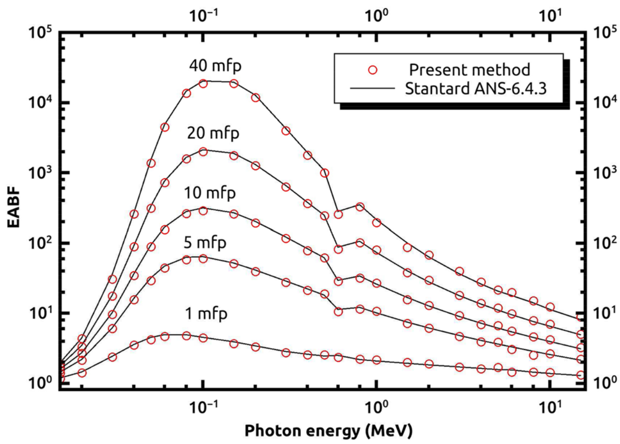

Fig. 1 EABF values of water using present method comparing with those of ANS-6.4.3 reference database up to 15 MeV photon energies and at 1, 5, 10, 20, 40 mfp

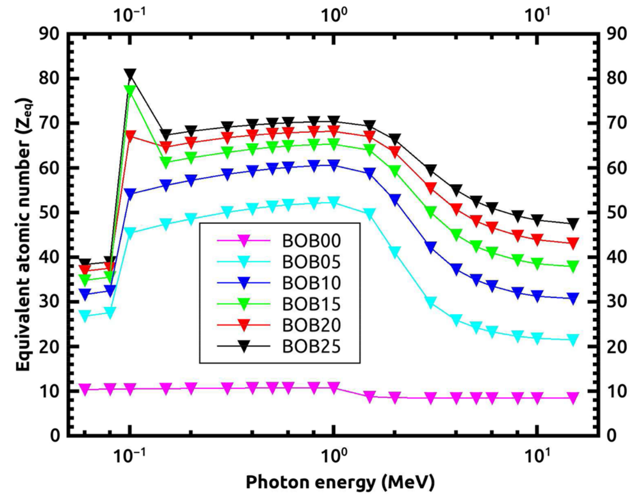

Fig. 2 Equivalent atomic numbers of bismuth borate glass systems as a function of photon energy

observed. This comparative approach has revealed that our results of gamma-ray buildup factors for the chosen glasses will be with negligible uncertainties.

4 Results and discussion

Table 1 shows the chemical structure and the density of the selected glasses. From Table 1, it is noted that the density of the glass samples increases with increasing the weight fraction of Bi. In addition, the glass samples are coded according to surplus the content Bi_2O_3 ascendingly as BOB00, BOB05, BOB10, BOB15, BOB20, and BOB25. For example, BOB00 means that the glass sample has 0 mol% Bi_2O_3 and BOB25 means 25 mol% Bi_2O_3. The equivalent atomic number (Z_{eq}) of these glasses is represented in Fig. 2. It is clear that the Z_{eq} values vary with photon energy and chemical composition of the glass. The behaviour of Z_{eq} with respect of photon energy is partly similar to the behaviour of effective atomic number (Z_{eff}) of multi-element materials. This phenomenon was discussed first by Hine [33], and then, it was supported by many authors for different materials [34, 35]. In addition, we expounded this phenomenon in the previous works for different materials [36, 37].

From Fig. 2, it is also seen that there are three distinguished regions of variations of the equivalent atomic number (Z_{eq}) depending on the incident photon energy–matter interactions. Furthermore, there are sudden jumps occur at low photon energies. These sudden jumps can be explained on the basis of k edge absorption of Bi at around 90.53 keV. The maximum value of Z_{eq} was found for bismuth borate glasses of BOB25 with 25 mol% Bi_2O_3. This can be explained on the basis of dependence of cross section of photoelectric process on the atomic number of elements as Z^{4-5}. The lowest weight fraction of Bi ($Z = 83$) present in the sample of BOB00 (0%) and the weight fraction of Bi are increased in the successive samples, and hence, Z_{eq} of the successive samples keeps on increasing. Finally, the maximum Z_{eq} was observed to correspond to bismuth borate glasses of BOB25, since this sample contains the highest weight fraction of Bi (62.12%).

The calculated values of EABF and EBF as a function of photon energy at chosen penetration depths (1, 10, 20, 30, and 40 mfp) are shown in Figs. 3 and 4, respectively, for all the glass samples. From these figures, one can distinguish three distinct zones of gamma-ray buildup factors with respect to the photon energy.

These zones are related to the main absorption and scattering processes of photon with matter. In the low energies, the EABF and EBF values were small due to the absorption processes (photoelectric effect) which play a major role to soak up the photon from the medium (say glass), and consequently, EABF and EBF values are reduced. Similarly, in the high energies, another photon absorption process, that is pair production, is the dominant one. In the intermediate energies, Compton scattering is the dominant process of photon interaction that only helps in degradation of photon energy due to scattering and fails to completely remove the photon [38]. Therefore, more the life time of the photon is long, more the probability of photon to escape the material is important. This process results in increasing the values of the EABF and EBF. One can observe a sharp peak in EABF and EBF, at very high energy, and large penetration depth. This is due to build up of secondary gamma photons produced by electron–positron annihilation in the medium due to multiple

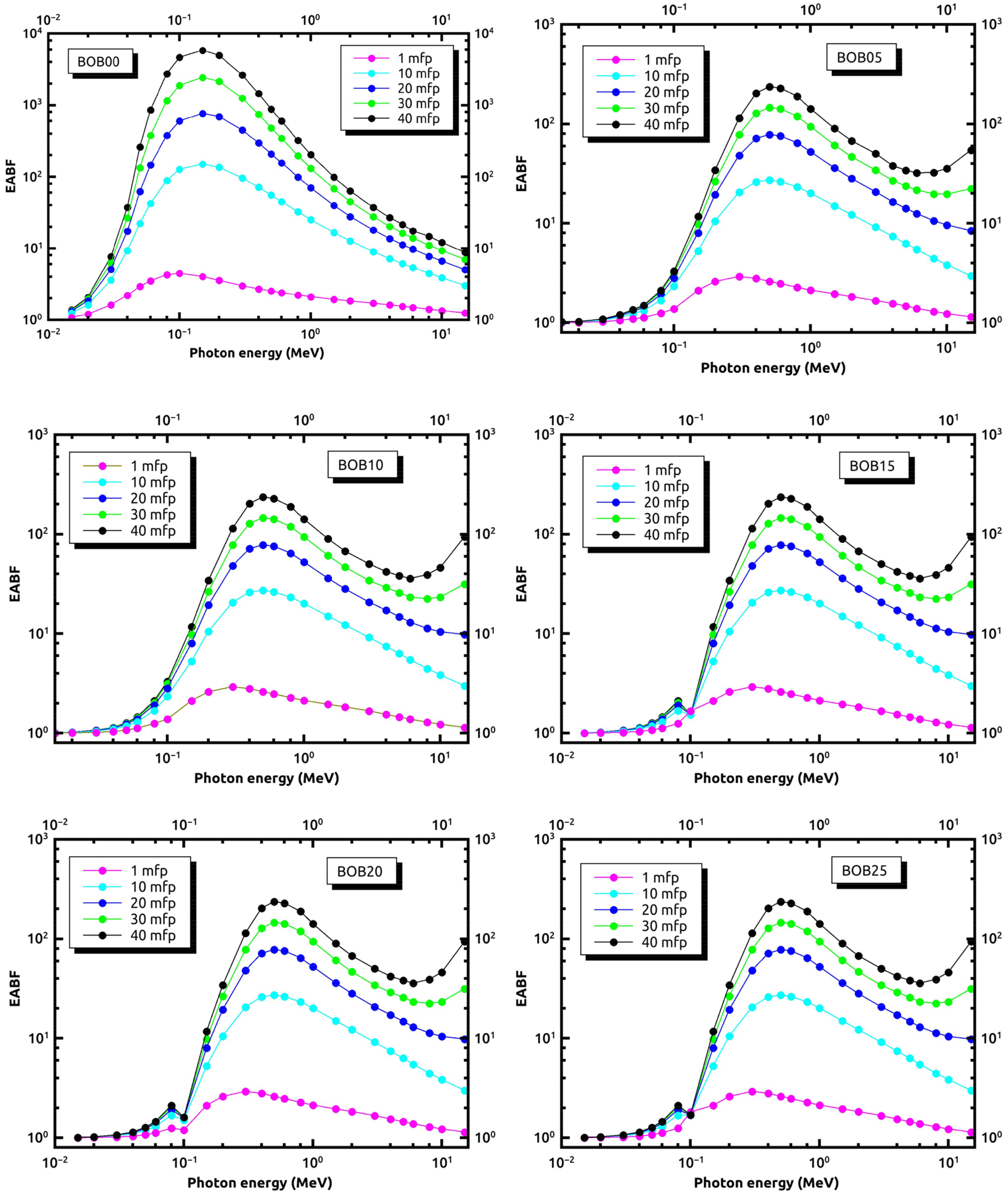

Fig. 3 EABF as a function of photon energy and at different penetration depths for bismuth borate glass systems

scattering events. In fact, the increase in penetration depth of the materials leading to increase the thickness of the interacting material which in turn results in increasing the scattering events in the interacting medium, in particular for the material with the highest equivalent atomic number. Hence, it results in large EABF and EBF values.

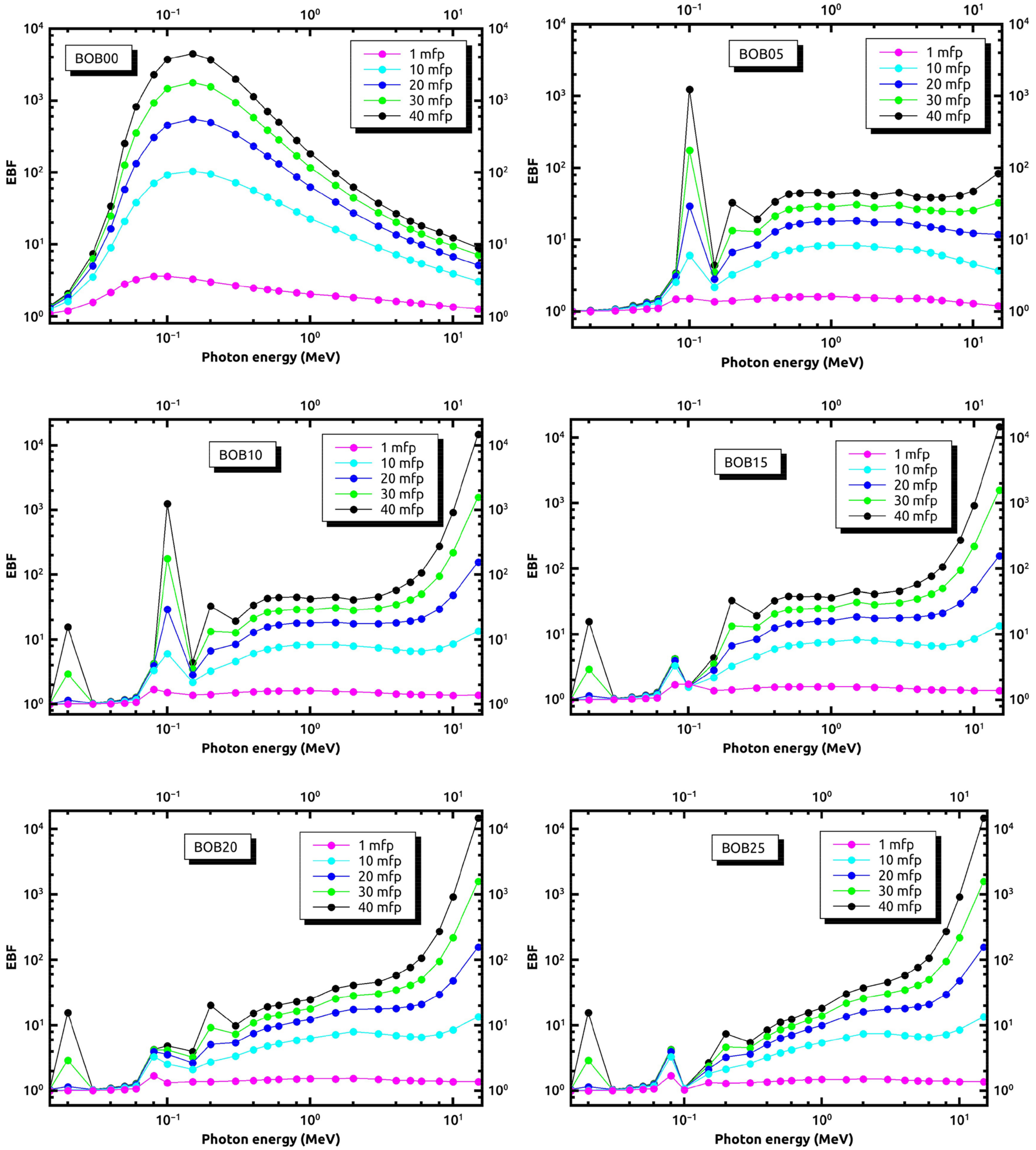

Fig. 4 EBF as a function of photon energy and at different penetration depths for bismuth borate glass systems

To take a close look to the previous results and the chemical composition dependency for the glasses under investigation, we plotted EBF values as a function of penetration depth for all glasses at (a) 0.015 MeV and (b) 1.5 MeV, as shown in Fig. 5. It is clear that all of the selected glasses with different concentrations of Bi_2O_3 have similar behaviour with respect to the penetration depth. The EBF values increase with increasing the penetration depth and the molar concentration of Bi_2O_3 at low photon energies (0.015 MeV, Fig. 5a). However, as photon energy increases

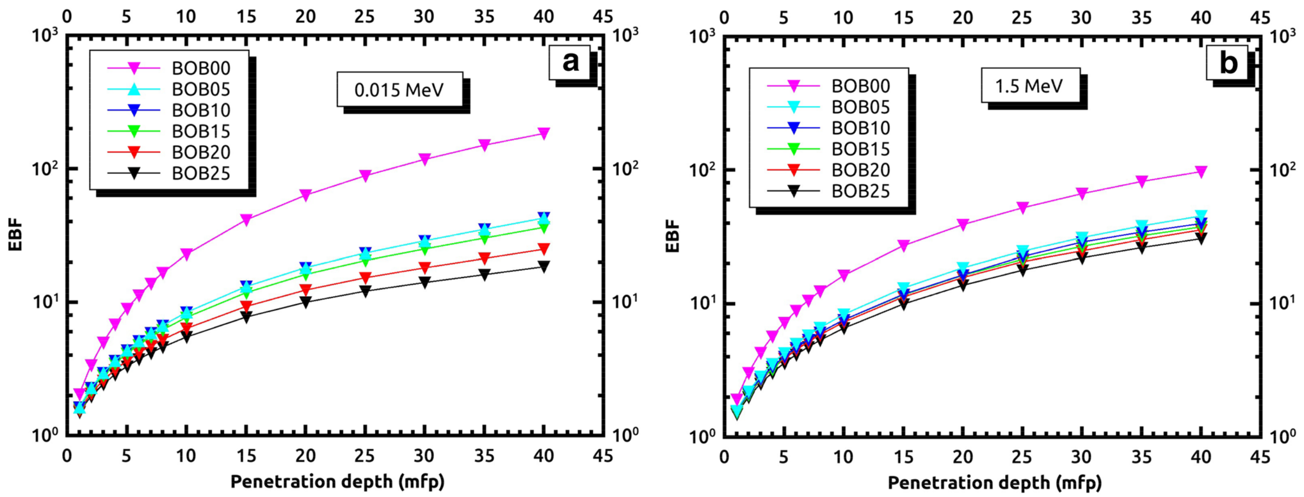

Fig. 5 EBF of bismuth borate glass systems as a function of penetration depth at **a** 0.015 MeV and **b** 1.5 MeV photon energies

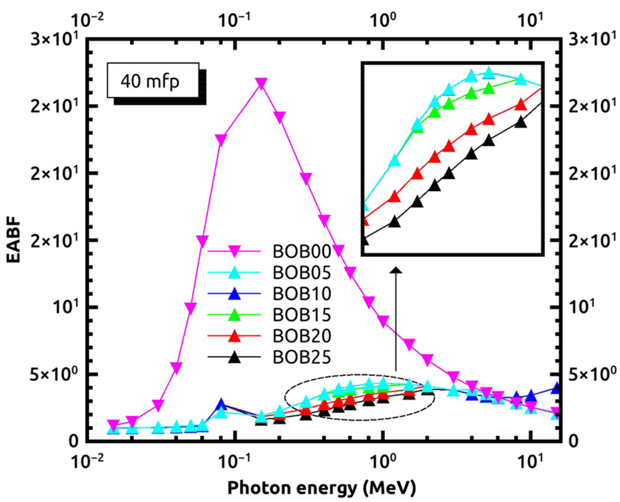

Fig. 6 EABF of bismuth borate glass systems as a function of photon energy at 40 mfp

(1.5 MeV, Fig. 5b), all of the glass samples are found to be semi-independent on the concentration of Bi_2O_3. This can be explained by the number of photons which raises from Compton scattering and from pair annihilation process (i.e., at high energies the absorption processes are too scarce). Figure 6 represents the EABF values for all of the glasses at 40 mfp over a wide range of energies between 0.015 and 15 MeV. It is obvious that the addition of Bi_2O_3 reduces EABF values mostly in the intermediate energies (0.04–1 MeV). For example, the BOB25 glass with 25 mol% Bi_2O_3 contains the largest molar concentration of Bi (62.1%), while the BOB05 glass with 5 mol% contains the smallest molar concentration of Bi (23.5%). Therefore, the increase of Bi concentration is responsible for increasing the Z_{eq} leading to decrease the values of EABF among all of the glass samples [39].

Furthermore, Figs. 2, 5, and 6 show that the largest values of EABF and EBF were observed for BOB00 which possesses a minimum Z_{eq}, whereas minimum values of EABF and EBF were observed for BOB25 which possesses a maximum Zeq. This may be due to the fact that BOB00 has low Z_{eq}, because it contains B ($Z = 5$, weight fraction = 0.234618), O ($Z = 8$, weight fraction = 0.601839), Na ($Z = 11$, weight fraction = 0.066522), Al ($Z = 13$, weight fraction = 0.039036) and Ca ($Z = 20$, weight fraction = 0.057984), while BOB25 contains high Z-element, i.e., Bi ($Z = 83$ weight fraction = 0.621213) in addition to B, O, Na, Al, and Ca.

Finally, despite the strong resemblance between the behaviour of EABF and EBF relating to the photon energy and penetration depth, significant discrepancies were noticed between the two notions at some photon energies. Figure 7 shows a comparison of energy absorption and exposure buildup factors for all of the glass samples over a continuous photon energy range at 10 mfp. It was found that the highest differences were in the intermediate photon energies. This is attributed to that a large number of scattered photons comes from Compton scattering and accumulate (buildup) in this region. It can also be seen that in the most of the photon energies, the EABF values are higher than those of EBF and this is due to the studied glasses that have higher Z_{eq} than those of the air. Therefore, the deposited energy in the medium (EABF) should be more than the deposited energy in the air (EBF). On the other hand, in some energies, the EBF values are higher than those of EABF. Consequently, the obtained results are expected to be useful in initial evaluation of where maximum radiation takes place, whether at the surface of the glass or inside the glass.

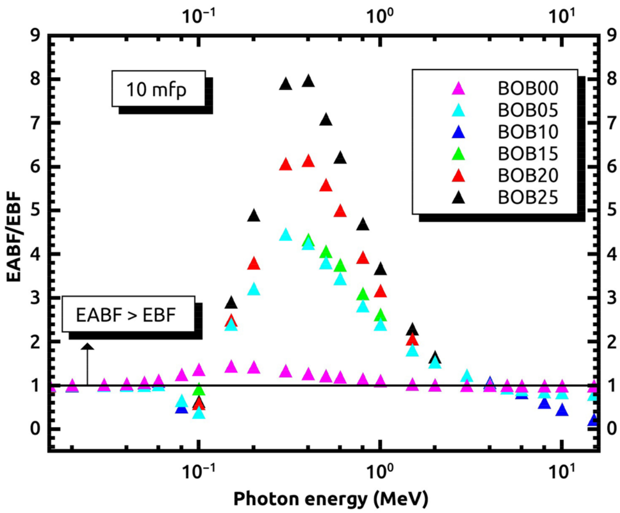

Fig. 7 Comparison between EABF and EBF of bismuth borate glass systems in the energy region 0.015–15 MeV at 10 mfp

5 Conclusion

In the present work, the gamma-ray buildup factors of bismuth borate glasses with different molar concentrations of Bi_2O_3 were calculated using (G–P) fitting method in the energy region 0.015–15 MeV up to a penetration depth of 40 mpf. It was noted that Z_{eq}, EABF, and EBF values are depend on incident photon energy as well as chemical composition of the glasses. Besides, EABF and EBF possess maximum values in the intermediate energy region, where Compton scattering is the dominant photon interaction process. It was found that BOB25 glass with 25 mol% of Bi_2O_3 has the lowest values of EABF and EBF; thus, it has a superior ability as shielding material against gamma ray. The obtained results provide scientific information to design the chosen glasses for gamma-ray shielding applications and to synthesize new materials for various applications in nuclear engineering and technologies.

References

1. W. Abd-Allah, H. Saudi, K.S. Shaaban, H. Farroh, Appl. Phys. A **125**(4), 275 (2019)
2. M. Kurudirek, N. Chutithanapanon, R. Laopaiboon, C. Yenchai, C. Bootjomchai, J. Alloys Compd. **745**, 355 (2018)
3. M. Kurudirek, J. Alloys Compd. **727**, 1227 (2017)
4. Y. Rammah, M. Sayyed, A. Abohaswa, H. Tekin, Appl. Phys. A **124**(9), 650 (2018)
5. G. Lakshminarayana, M. Sayyed, S. Baki, A. Lira, M. Dong, K.M. Kaky, I. Kityk, M. Mahdi, Appl. Phys. A **124**(5), 378 (2018)
6. M. Dong, O. Agar, H. Tekin, O. Kilicoglu, K.M. Kaky, M. Sayyed, Compos. Part B Eng. **165**, 636 (2019)
7. H. Gomaa, M. Sayyed, H. Tekin, G. Lakshminarayana, A. EL-Dosokey, Phys. B Condens. Matter **1**, 4 (2018). https://doi.org/10.1016/j.physb.2018.11.011
8. G. Lakshminarayana, M. Sayyed, S. Baki, A. Lira, M. Dong, K.A. Bashar, I. Kityk, M. Mahdi, J. Electron. Mater. **48**(2), 930 (2019)
9. M. Almatari, Radiochim. Acta
10. M. Sayyed, K.M. Kaky, M. Mhareb, A.H. Abdalsalam, N. Almousa, G. Shkoukani, M.A. Bourham, Radiati. Phys. Chem. (2019)
11. Y. Rammah, A. Ali, R. El-Mallawany, A. Abdelghany, J. Mol. Struct. **1175**, 504 (2019)
12. Y. Rammah, M. Sayyed, A. Ali, H. Tekin, R. El-Mallawany, Appl. Phys. A **124**(12), 832 (2018)
13. K.M. Kaky, M. Sayyed, F. Laariedh, A.H. Abdalsalam, H. Tekin, S. Baki, Appl. Phys. A **125**(1), 32 (2019)
14. H. Tekin, E. Kavaz, E. Altunsoy, O. Kilicoglu, O. Agar, T. Erguzel, M. Sayyed, Ceram. Int. (2019)
15. W. Marltan, P.V. Rao, H. Tekin, M. Sayyed, R. Klement, D. Galusek, G. Lakshminarayana, P.S. Prasad, N. Veeraiah, Ceram. Int. **45**(6), 7619 (2019)
16. U. Fano, Nucleon. (US) Ceased Publ. **11** (1953)
17. V.P. Singh, N. Badiger, T. Chanthima, J. Kaewkhao, Radiat. Phys. Chem. **98**, 14 (2014)
18. G.R. White, Phys. Rev. **80**(2), 154 (1950)
19. Y. Harima, Radiat. Phys. Chem. **41**(4–5), 631 (1993)
20. ANSI/ANS-6.4.3. Gamma ray attenuation coefficient and buildup factors for engineering materials (1991)
21. E. Kavaz, N.Y. Yorgun, J. Alloys Compd. **752**, 61 (2018)
22. A. Shimizu, T. Onda, Y. Sakamoto, J. Nucl. Sci. Technol. **41**(4), 413 (2004)
23. D. Sardari, A. Abbaspour, S. Baradaran, F. Babapour, Appl. Radiat. Isot. **67**(7–8), 1438 (2009)
24. H. Hirayama, J. Nucl. Sci. Technol. **32**(12), 1201 (1995)
25. M. Sayyed, B. Elbashir, H. Tekin, E. Altunsoy, D. Gaikwad, J. Phys. Chem. Solids **121**, 17 (2018)
26. V.P. Singh, N. Badiger, J. Kaewkhao, J. Non-Cryst. Solids **404**, 167 (2014)
27. M. Sayyed, S.I. Qashou, Z. Khattari, J. Alloys Compd. **696**, 632 (2017)
28. L. Gerward, N. Guilbert, K.B. Jensen, H. Leving, Radiat. Phys. Chem. **71**, 653 (2004)
29. M. Sayyed, M. AlZaatreh, K. Matori, H. Sidek, M. Zaid, Results Phys. **9**, 585 (2018)
30. M. Sayyed, J. Alloys Compd. **695**, 3191 (2017)
31. M. Sayyed, H. Elhouichet, Radiat. Phys. Chem. **130**, 335 (2017)
32. M. Sayyed, S.A. Issa, S.H. Auda, Prog. Nucl. Energy **100**, 297 (2017)
33. G. Hine, Phys. Rev. **85**, 725 (1952)
34. B. Oto, S.E. Gulebaglan, Z. Madak, E. Kavaz, Radiat. Phys. Chem. (2019)
35. M. Kurudirek, Radiat. Environ. Biophys. **55**(4), 501 (2016)
36. B.T. Tonguc, H. Arslan, M.S. Al-Buriahi, Radiat. Phys. Chem. **153**, 86 (2018)
37. M.S. Al-Buriahi, H. Arslan, B.T. Tonguc, Nucl. Sci. Tech. **30**(7), 15 (2019)
38. S. Manohara, S. Hanagodimath, L. Gerward, Radiat. Phys. Chem. **79**(5), 575 (2010)
39. S. Raut, V. Awasarmol, S. Shaikh, B. Ghule, S. Ekar, R. Mane, P. Pawar, Radiat. Effects Defects Solids **173**(3–4), 329 (2018)